

G24.78+0.08: A cluster of high-mass (proto)stars

R. S. Furuya¹, R. Cesaroni¹, C. Codella², L. Testi¹, R. Bachiller³, and M. Tafalla³

¹ Osservatorio Astrofisico di Arcetri, INAF, Largo E. Fermi 5, 50125 Firenze, Italy

² Istituto di Radioastronomia, CNR, Sezione di Firenze, Largo E. Fermi 5, 50125 Firenze, Italy

³ Observatorio Astronómico Nacional (IGN), Apartado 1143, 28800 Alcalá de Henares (Madrid), Spain

Received 6 May 2002 / Accepted 6 June 2002

Abstract. We present the results of high angular resolution observations at millimeter wavelengths of the high-mass star forming region G24.78+0.08, where a cluster of four young stellar objects is detected. We discuss evidence for these to be high-mass (proto)stars in different evolutionary phases. One of the sources is detected only in the continuum at 2 and 2.6 mm and we suggest it may represent a good candidate of a high-mass protostar.

Key words. stars: formation – radio lines: ISM – ISM: jets and outflows – ISM: individual objects: G24.78+0.08

1. Introduction

High-mass stars are usually defined as stars with mass above $\sim 8 M_{\odot}$: for zero-age main sequence (ZAMS) objects, this corresponds to a luminosity $\geq 5 \times 10^3 L_{\odot}$ and a spectral type earlier than B3. Such a definition is based on a basic theoretical result (Palla & Stahler 1993): unlike their low-mass equivalents, protostars with masses above $8 M_{\odot}$ are expected to evolve on timescales much shorter than those relevant to accretion. As a consequence, they reach the ZAMS still deeply embedded in their parental clouds. Consequently, the dusty parental cocoon makes difficult to observe the newly born stars which can be studied only in the IR or at longer wavelengths. Moreover, massive stars form in clusters, which not only complicates the observations of each single young stellar object (YSO), but also profoundly affects the surrounding environment: copious production of Lyman continuum photons eventually leads to the destruction of the parental cloud thus making impossible to trace back the formation process.

Notwithstanding these difficulties, in recent years much progress has been done to identify earlier and earlier stages in the evolution of massive stars (see e.g. Kurtz et al. 2000). This eventually resulted in a scenario according to which high-mass star formation would proceed in dense, massive cores $\lesssim 0.1$ pc in size: as time goes on, the temperature of such cores would increase and the original spherical symmetry would change into a more axisymmetric structure; the embedded stars would develop circumstellar disks and bipolar outflows along the disk axes, which would allow expansion of the ultracompact (UC) HII regions created by the Lyman continuum of the stars. Given the relatively large number of hot cores and UC HII regions

revealed to date, the latest phases of such a scenario are quite well assessed; as opposite, we still have a limited understanding of the very earliest stages, prior to the arrival onto the ZAMS. Massive YSOs of this type may be considered the equivalent of class 0 low-mass YSOs, namely protostars still in the main accretion phase. No iron clad evidence for the existence of high-mass protostars has been presented so far, but a few candidates have been detected (Hunter et al. 1998; Molinari et al. 1998).

Here, we present the results of a study of the massive star forming region G24.78+0.08. This region has been selected from a sample of OH/H₂O maser sources identified by Forster & Caswell (1989) and it was observed by Codella et al. (1997, hereafter CTC) in the NH₃(2, 2) and (3, 3) inversion transitions. One interesting feature of G24.78+0.08 is the presence of two groups of maser spots: one, close to an UC HII region, consists of both OH and H₂O masers, whereas the other, offset by $\sim 8''$ to the NE, contains only H₂O masers. Both groups are embedded in a ~ 0.5 pc clump traced by the ammonia emission. This situation resembles very closely that of the W3(H₂O)/W3(OH) system, where a high-mass YSO has been found in association with W3(H₂O) (Turner & Welch 1984), whereas W3(OH) coincides with an UC HII region created by an early-type star. We have hence decided to search for a possible source associated with the isolated H₂O group in G24.78+0.08. To this purpose, we have studied the continuum and line emission from this region at various wavelengths. The basic results are illustrated in the following, while a more detailed description is postponed to a subsequent paper.

2. Observations

In 1998–2002, we carried out continuum emission imaging using the Nobeyama Millimeter Array (NMA) at 2 mm, the Plateau de Bure interferometer (PdBI) at 2.6 mm, and

Send offprint requests to: R. Cesaroni,
e-mail: cesa@arcetri.astro.it

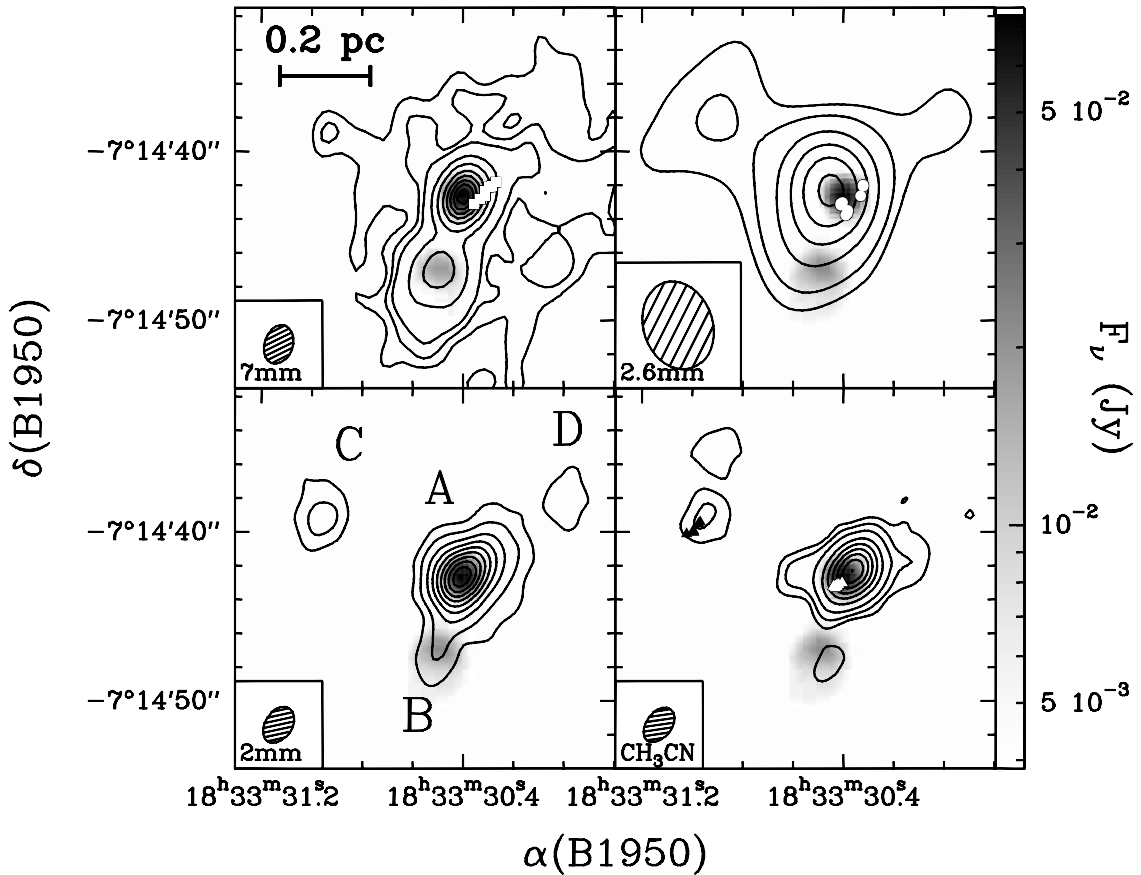


Fig. 1. Overlay of the 1.3 cm continuum image of CTC (grey scale) with the maps (contours) of the 7 mm (top left panel), 2.6 mm (top right), and 2 mm continuum (bottom left), and CH₃CN(8–7) line (bottom right) emission. Circles, squares, and triangles represent respectively CH₃OH (Walsh et al. 1998), OH and H₂O (Forster & Caswell 1999) maser spots. Contour levels are as follows: 0.5, 0.9, 1.5, 6, and 15 to 90 in steps of 15 mJy/beam for the 7 mm map; 15 and 30 to 150 in steps of 30 mJy/beam for the 2.6 mm map; 7 and 17 to 122 in step of 15 mJy/beam for the 2 mm map; 70, 120, and 220 to 1420 in steps of 200 mJy/beam for the CH₃CN map. The 3σ RMS sensitivities are 0.45, 11, 7.6, and 82 mJy/beam for the 7, 2.6, and 2 mm continuum and the CH₃CN line maps, respectively. The letters mark the four objects detected in the region (see text).

Very Large Array (VLA) in the D-array configuration at 7 mm. The NMA observations were performed together with the enhanced Rainbow mode using the 45-m telescope as one of the array elements. At 2 and 2.6 mm, we observed lines of CH₃CN(8–7) and ¹²CO(1–0), respectively. The resulting synthesised beam sizes were 2′′.3×1′′.6 at 2 mm, 5′′.3×4′′.1 at 2.6 mm, and 2′′.3×1′′.7 at 7 mm. For all datasets the inner hole in the (u, v) plane has a radius in the range 4.5 to 6.5 $k\lambda$. Attained sensitivities in individual maps are described in the caption of Fig. 1.

3. Results and discussion

Our main findings are illustrated in Figs. 1 and 2. The former shows the maps of the continuum emission from 2 to 7 mm and the integrated intensity map of the CH₃CN(8–7) $K = 0$ and 1 line emission overlaid to the 1.3 cm continuum map of CTC. Also shown are the positions of the OH and H₂O maser spots from Forster & Caswell (1999) and those of the CH₃OH masers from Walsh et al. (1998). The most important result is the detection of four separate sources, which are best seen in the 2 mm continuum map: these have been identified

with letters A to D. Of these, A and B were already detected by CTC and are associated with two compact HII regions (see also Forster & Caswell 2000). Source C is seen in the mm continuum and CH₃CN line maps: this confirms our expectation that the H₂O masers to the NE were associated with a compact molecular core. A surprising result is the detection at 2 and 2.6 mm of a continuum peak, D, to the NW of the UC HII region in A. This must trace a compact dusty core, which is not detected in any of the molecular lines observed: such a lack of line emission may be indicative of molecular depletion and hence high density and low temperature.

Figure 2 presents maps of the blue- and red-shifted emission in the wings of the ¹²CO(1–0) line: these reveal two bipolar outflows centred on A and C. It is thus likely that one of the flows originates from the early-type star ionising the UC HII region in A, while the other may be powered by a deeply embedded YSO in C. The parameters of the outflow can be derived as usual by integrating the emission under the line wings and assuming an age equal to the kinematical time scale (2×10^4 yr) given by the ratio between the size of the lobes (0.45 pc) and the maximum velocity reached in the flow (20 km s⁻¹): we find very similar values for both outflows, corresponding to masses

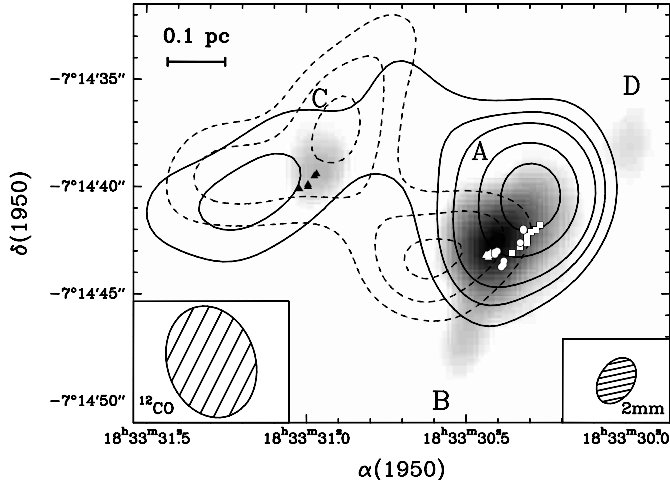


Fig. 2. Overlay of the 2 mm continuum image (grey scale) with the outflow maps (contours) obtained by integrating the $^{12}\text{CO}(1-0)$ line emission under the wings, from 90 to 105 km s^{-1} (full contours) and from 116 to 131 km s^{-1} (dashed contours). The cloud LSR velocity is $\sim 111 \text{ km s}^{-1}$. Contour levels correspond to 1.1, 1.4, and 1.7 Jy/beam (dashed contours) and 0.4, 0.6, 0.8, 1.2, and 1.6 Jy/beam (full contours). Symbols and letters have the same meaning as in Fig. 1.

of $\sim 10 M_{\odot}$, mechanical luminosities of $\sim 10 L_{\odot}$, and mass loss rates of $\sim 5 \times 10^{-4} M_{\odot} \text{ yr}^{-1}$. Such values are to be taken as lower limits, as the $^{12}\text{CO}(1-0)$ line may be optically thick and the lobes might extend over a larger region than that imaged by the interferometer. Also, correcting for the (unknown) inclination of the outflow axis would increase the real velocity and hence the mass loss rate and mechanical luminosity. We conclude that the values quoted above are typical of high-mass stars, as one can see e.g. from Table 1 of Churchwell (1997).

Finally, it is worth noting that the two outflow axes are parallel to the direction outlined by the maser spots: this result leads support to the belief that H_2O masers could be strongly associated with outflows (see Felli et al. 1992), as already pointed out by CTC.

Three cores (A, C, D) and two compact HII regions (A and B) are seen towards G24.78. Now, we try to shed light on the nature of these objects. In Fig. 3, we plot their continuum spectra obtained by adding the 6 cm and 3.6 cm measurements of Becker et al. (1994) and Forster & Caswell (2000) to our data. The four spectra have been fitted with a simple model consisting of an HII region surrounded by a dusty core: spherical symmetry and constant density and temperature have been assumed. We adopted a dust absorption coefficient $\kappa(\nu) = 0.005 \text{ cm}^2 \text{ g}^{-1} (\nu/231 \text{ GHz})^2$ (following Preibisch et al. 1993; Molinari et al. 2000). The flux depends on the radius (R_{HII}) and emission measure (EM) of the HII region, and only on the mass (M_{core}) and temperature (T_{dust}) of the surrounding core because at $\lambda \geq 2 \text{ mm}$ the thermal emission from dust is optically thin. In order to minimise the number of free parameters, we have used the results of the present work and of CTC to fix the diameters of the HII regions in A and B and the temperatures of the cores in A and C. Under these assumptions, we estimated the emission measure of the HII regions and the mass of the cores in A and C: in the other cases only

Table 1. Parameters for the fits in Fig. 3. An electron temperature of 10^4 K and a distance of 7.7 kpc have been assumed.

| Source | R_{HII} (pc) | EM (pc cm^{-6}) | T_{dust} (K) | M_{core} (M_{\odot}) |
|--------|--------------------------|---------------------------------|--------------------------|--------------------------------------|
| A | 0.005 ^(a) | $2 \cdot 10^9$ | 90 ^(a) | 550 |
| B | 0.05 ^(a) | $6.5 \cdot 10^6$ | 90 ^(b) | ≤ 40 |
| C | < 0.005 ^(c) | $> 9 \cdot 10^6$ | 30 ^(a) | 250 |
| D | < 0.005 ^(c) | $> 7.5 \cdot 10^6$ | ≤ 30 ^(d) | ≥ 100 |

^(a) Derived by CTC.

^(b) No T_{dust} estimate: same temperature as in A assumed.

^(c) Upper limit assumed equal to diameter of HII region in A.

^(d) Assumed equal or less than the temperature of core C.

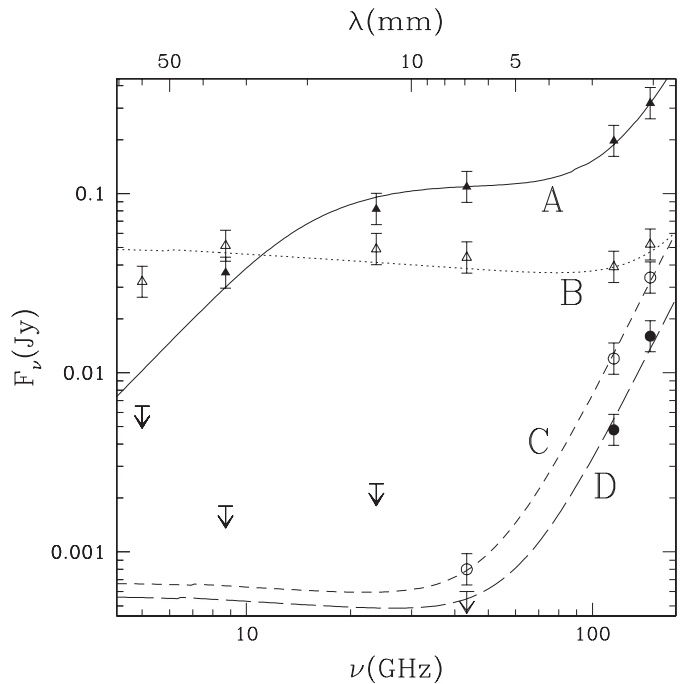


Fig. 3. Spectrum of the continuum emission of the four objects detected towards G24.78+0.08. The letters identify each spectrum according to the notation in Fig. 1. The lines are fits to the data obtained with the model described in the text and for the parameters listed in Table 1.

limits can be set. The fit parameters are given in Table 1. For core D we have assumed a maximum temperature equal to that of core C. Although such an assumption is arbitrary, it seems unlikely that the gas is hotter, otherwise one would expect to detect line emission from molecules evaporated from grain mantles: as discussed above, such emission is not seen at the same level as in A and C.

4. Nature of the sources and evolutionary sequence

In the light of the previous results, we can now discuss the nature of the four sources, whose properties are schematically summarised in Table 2.

B The negligible molecular line emission seen towards this object indicates that the HII region has already expanded

Table 2. Characteristics of the four objects observed.

| YSO | D | C | A | B |
|---|---|---|---|---|
| Dusty Core (mm cont.) | Y | Y | Y | N |
| Molecular Core (NH ₃ , CH ₃ CN) | N | Y | Y | N |
| Bipolar Outflow (¹² CO) | N | Y | Y | N |
| H ₂ O masers | N | Y | Y | N |
| CH ₃ OH masers | N | N | Y | N |
| OH masers | N | N | Y | N |
| UC HII region (cm free-free) | N | N | Y | Y |

destroying the densest portion of the molecular surroundings. The ionising star is hence relatively old, although less than $\sim 10^5$ yr, the expected life time of UC HII regions (Wood & Churchwell 1989).

- A The UC HII region is unresolved at 1.3 cm (CTC) and deeply embedded in a dense molecular core, as witnessed by the absorption detected in the NH₃(2, 2) and (3, 3) lines. The compactness of the ionised region, the temperature and mass of the surrounding core, the existence of a bipolar outflow, the strong emission in rare molecules such as CH₃CN, the presence of maser emission in various species all indicate that we are dealing with a young early-type ZAMS star strongly interacting with the surrounding environment and in an earlier evolutionary phase than the star in B.
- C The basic difference with respect to A which suggests a younger age for C is represented by the absence of an UC HII region toward C even though the large mass of the molecular core, the outflow parameters, and the detection of hot core species such as CH₃CN are all typical of high-mass YSOs. This conclusion is also supported by the fact that C, unlike A, harbours *only* H₂O maser emission: the common belief is that H₂O masers should appear at a very early stage of the evolution of a high-mass star, which also suggests that C is younger than A. Further evidence in favour of C being associated with massive YSOs is represented by the large mass of the core, $\sim 250 M_{\odot}$. In fact, such a mass is comparable to that of cores hosting high-mass YSOs (see Table 1 of Kurtz et al. 2000); moreover, it is contained in 0.07 pc and is ~ 6 times greater than that (40 M_{\odot} over 0.2 pc) of the low-mass star forming clumps observed by Testi et al. (1998) in the Serpens region. Therefore, it is unlikely that we are observing a low-mass star forming core.

D This is the most intriguing object, as it is traced only by the millimeter continuum emission and is not detected in any molecular species (CO, CH₃CN, NH₃). One cannot rule out the possibility that this is a quiescent core without star formation. However, this is hard to believe given the large value of the mass, $>100 M_{\odot}$: as already discussed for C, values such large are not appropriate for low-mass star forming cores.

In conclusion, we have detected a cluster containing at least 4 high-mass YSOs, in different evolutionary phases. More precisely, the ages of these YSOs are likely to be in the order $t_B > t_A > t_C > t_D$. We suggest that core D represents an excellent candidate for a high-mass protostar.

Acknowledgements. It is a pleasure to thank the staff of IRAM, NRAO, and NRO for their help during the observations. Special thanks are due to Prof. Sachiko Okumura for taking care of our observations with the Nobeyama Millimeter Array.

References

- Becker, R. H., White, R. L., Helfand, D. J., & Zoonematkermani, S. 1994, *ApJS*, 91, 347
- Churchwell, E. 1997, in *Herbig-Haro Flows and the Birth of Stars*, ed. B. Reipurth, & C. Bertout (Kluwer Academic Publishers), IAU Symp., 182, 525
- Codella, C., Testi, L., & Cesaroni, R. 1997, *A&A*, 325, 282 (CTC)
- Felli, M., Palagi, F., & Tofani, G. 1992, *A&A*, 255, 293
- Forster, J. R., & Caswell, J. L. 1989, *A&A*, 213, 339
- Forster, J. R., & Caswell, J. L. 1999, *A&AS*, 137, 43
- Forster, J. R., & Caswell, J. L. 2000, *ApJ*, 530, 371
- Hunter, T. R., Neugebauer, G., Benford, D. J., et al. 1998, *ApJ*, 493, L97
- Kurtz, S., Cesaroni, R., Churchwell, E., Hofner, P., Walmsley, C. M. 2000, *Protostars and Planets IV*, ed. V. Mannings, A. Boss, & S. Russel (Tucson: Univ. of Arizona Press)
- Molinari, S., Testi, L., Brand, J., Cesaroni, R., & Palla, F. 1998, *ApJ*, 505, L39
- Molinari, S., Brand, J., Cesaroni, R., & Palla, F. 2000, *A&A*, 355, 617
- Palla, F., & Stahler, S. W. 1993, *ApJ*, 418, 414
- Preibisch, Th., Ossenkopf, V., Yorke, H. W., & Henning, Th. 1993, *A&A*, 279, 577
- Testi, L., Sargent, A. I., Olmi, L., & Onello J. S. 2000, *ApJ*, 540, L53
- Turner, J. L., & Welch, W. J. 1984, *ApJ*, 287, L81
- Walsh, A. J., Burton, M. G., Hyland, A. R., & Robinson, G. 1998, *MNRAS*, 301, 640
- Wood, D. O. S., & Churchwell, E. 1989, *ApJ*, 340, 265